

Entanglement dynamics in a model tripartite quantum system

Pradip Laha, B. Sudarsan, S. Lakshmibala[†] and
V. Balakrishnan

Department of Physics, Indian Institute of Technology Madras, Chennai 600 036,
India

Abstract.

A system comprising a Λ -type or V-type atom interacting with two radiation fields exhibits, during its dynamical evolution, interesting optical phenomena such as electromagnetically-induced transparency (EIT) and a variety of nonclassical effects. Signatures of the latter are seen in the entanglement dynamics of the atomic subsystem and in appropriate field observables. Some of these effects have been experimentally detected, and have even been used to change the nonlinear optical properties of certain atomic media. It is therefore useful to investigate the roles played by specific initial states of the radiation fields, detuning parameters, field nonlinearities and the nature of field-atom couplings on EIT and on the entanglement between subsystems. We investigate these aspects in the framework of a simple model that captures the salient features of such tripartite entangled systems. Entanglement dynamics is shown to be very sensitive to the intensity-dependent atom-field couplings. Unexpected interesting features pertaining to the collapses and revivals of the atomic subsystem von Neumann entropy appear. These features could, in principle, be useful in enabling entanglement.

PACS numbers: 42.50.-p, 03.67.-a, 03.67Mn, 42.50Dv, 42.50Md

1. Introduction

Interacting quantum systems exhibit many interesting features during temporal evolution. These include diverse nonclassical effects such as quantum entanglement, revival phenomena [1–4], collapse of the measure of entanglement to a constant value over certain time intervals, and so on. Atom optics provides a convenient framework for examining these effects. In tripartite entangled systems comprising an atom interacting with two radiation fields, further effects can occur, such as electromagnetically-induced transparency (EIT): the appearance, under suitable conditions, of a transparency window within the absorption spectrum of the atomic system. Apart from the change in the transmission coefficient, atomic media can also exhibit interesting dispersive properties as a consequence of EIT. This feature has been exploited to create materials

[†] Author to whom any correspondence should be addressed.

that demonstrate slow light-pulse propagation and enhanced nonlinear optical properties (for a review, see [5]).

Extensive experimental investigations on EIT have been carried out on three-level atoms interacting with a probe field and a coupling field. Following the report on the occurrence of EIT in optically opaque Sr^+ vapour in 1991 [6], several detailed experiments have been performed on the nature of this optical phenomenon in various atom-field configurations (see, e.g., [7, 8]). In the absence of the coupling field, the intensity of the probe field (equivalently, the corresponding mean photon number) will remain nearly constant over a small range of values of the detuning parameter about zero. The transparency window created by the coupling field in this absorption spectrum is signalled by the appearance of a peak in the probe field intensity. It is therefore reasonable to expect that, if the entangled tripartite system displays collapses and revivals of the probe intensity during time evolution, this peak should be seen at any instant lying in a time interval in which the mean photon number of the probe field collapses to a constant value in the absence of the coupling field.

In tripartite systems comprising a V-type or Λ -type atom and two radiation fields, the inclusion of Kerr-type nonlinearities in the field subsystem opens up the possibility of collapses and revivals of the mean photon number corresponding to either field, under specific conditions. EIT can therefore be investigated, for instance, at an instant in a time interval when the mean photon number collapses for the first time, independent of whether or not further collapses occur. On longer time scales the subsystem von Neumann entropy (SVNE) corresponding to the atom can collapse to a constant value over a sufficiently long time interval and this feature could possibly be mirrored in the temporal evolution of the mean photon number of a field subsystem. Further, the manner in which different initial field states, detuning parameters and interaction strengths affect both EIT and the entanglement dynamics on long time scales needs to be examined. Both Λ and V atoms interacting with a probe field and a coupling field are good candidates for theoretical and experimental investigations of all the foregoing aspects.

The revival phenomenon is exhibited even by a single-mode radiation field propagating in a Kerr-like medium, governed by an effective Hamiltonian of the form $a^\dagger a^2$, where a and a^\dagger are the photon annihilation and creation operators [2,3]. Fractional revivals occur at specific instants between two successive revivals of the initial wave packet, when the initial wave packet splits into two or more similar copies of itself [1]. Signatures of revivals and fractional revivals are captured by appropriate quadrature observables and their higher moments [9, 10]. Collapses and revivals are of greater interest, however, in bipartite and multipartite systems that involve interaction between the subsystems, entailing nontrivial entanglement dynamics. A bipartite model [11] of a multi-level atom interacting with a single-mode radiation field predicts [12] collapses and revivals of the state of the field (also reflected, in this case, in the temporal behaviour of the field SVNE), when the nonlinearity in the atomic medium is weak compared to the strength of atom-field interaction. For stronger nonlinearity, however, the revival

phenomenon is absent; a detailed time-series analysis of the mean photon number reveals a gamut of ergodicity properties displayed by this observable, ranging from regular to chaotic behaviour [13, 14].

Entanglement dynamics in the foregoing bipartite model turns out to depend significantly on the degree to which the initial state of the field departs from perfect coherence. This has been deduced by selecting, as initial field states, the family of photon-added coherent states (PACS) [15] denoted by $|\alpha, m\rangle$, where $\alpha \in \mathbb{C}$ and $m = 0, 1, 2, \dots$. The standard oscillator coherent state (CS)

$$|\alpha\rangle = e^{-|\alpha|^2/2} \sum_{n=0}^{\infty} \frac{\alpha^n}{\sqrt{n!}} |n\rangle \quad (1)$$

corresponds to the case $m = 0$, while the m -photon-added coherent state $|\alpha, m\rangle$ is obtained by normalising the state $(a^\dagger)^m |\alpha\rangle$ to unity. The set $\{|\alpha, m\rangle\}$ provides a family of states whose departure from coherence is precisely quantifiable. Experimental realisation of the single photon-added coherent state using quantum state tomography [16] has added to the relevance of these studies.

If the atom has only a very small number of energy levels, the dynamics of entanglement differs both qualitatively and quantitatively from that of the bipartite model discussed above. This aspect has been studied [17, 18] in the framework of a three-level V or Λ atom interacting with a single-mode radiation field. A striking feature is that, relatively independent of the degree of coherence of the initial state of the radiation field, the photon number statistics and the degree of entanglement are affected strongly by the low dimensionality of the atomic Hilbert space. This feature continues to hold good for tripartite extensions of the model in which the atom interacts with two radiation fields.

This tripartite model is most suitable for our present purposes, as it provides a convenient framework for examining EIT, both on short time scales when the mean photon number records its first collapse, and on longer time scales where the measure of entanglement between the atom and fields remains constant over a significant time interval [17], for appropriate choices of the field state and parameter values. Another important aspect we study is the role played by intensity-dependent couplings in entanglement dynamics. It has been found [19] that, for an intensity-dependent coupling of the form $(a^\dagger a)^{1/2}$ between an initial CS and a Jaynes-Cummings atom, the mean photon number can be evaluated in closed form, and the mean photon energy undergoes periodic collapses and revivals in this case. Subsequent studies have been carried out on the dynamics of the Jaynes-Cummings atom interacting through an intensity-dependent coupling with other initial states of the radiation field such as the squeezed vacuum and the $SU(1, 1)$ coherent state [20, 21]. A coupling proportional to $1/(a^\dagger a)^{1/2}$ has also been used [22] in a tripartite model, motivated by the fact that this form arises naturally in the context of diagonal-state representations of the density matrix in a restricted Hilbert space where the zero-photon state is absent [23]. An intensity-dependent coupling of the form $(1 + \kappa a^\dagger a)^{1/2}$, $0 \leq \kappa \leq 1$ has been shown [24] to lead to a closed-form expression for

the mean photon energy. Here $\kappa = 0$ reduces to the Heisenberg-Weyl algebra for the field operators, while $\kappa = 1$ leads to the $SU(1, 1)$ algebra for (nonlinear combinations of) these operators [25]. Intermediate values of κ corresponds to a deformed $SU(1, 1)$ operator algebra. While the revival phenomenon has been examined in several models with intensity-dependent couplings, including the tripartite system of an atom interacting with two radiation fields [26, 27], the effect of such a coupling on the entanglement dynamics and on EIT has not been investigated. In this paper, we report on the effects of a general intensity-dependent coupling of the form $(1 + \kappa a^\dagger a)^{1/2}$ on these two phenomena in the tripartite model of a Λ atom interacting with two radiation modes. We have also investigated the corresponding case of a V atom. We do not present those results, as they are not qualitatively different in any significant manner from those for the Λ atom.

2. Λ atom interacting with two radiation modes

The tripartite model has two radiation fields: a ‘probe field’ F_1 and a ‘coupling field’ F_2 , of respective frequencies Ω_1 and Ω_2 , with annihilation and creation operators a_i and a_i^\dagger ($i = 1, 2$). The highest energy state of the Λ atom is denoted by $|3\rangle$, and $|1\rangle$ and $|2\rangle$ are the two lower energy states. F_1 and F_2 induce, respectively, the $|1\rangle \leftrightarrow |3\rangle$ and $|2\rangle \leftrightarrow |3\rangle$ transitions, while the transition $|1\rangle \leftrightarrow |2\rangle$ is dipole-forbidden. The general Hamiltonian that incorporates field nonlinearities and intensity-dependent couplings is given (setting $\hbar = 1$) by

$$H = \sum_{j=1}^3 \omega_j \sigma_{jj} + \Omega_1 a_1^\dagger a_1 + \chi_1 a_1^{\dagger 2} a_1^2 + \Omega_2 a_2^\dagger a_2 + \chi_2 a_2^{\dagger 2} a_2^2 + \lambda_1 (R_1 \sigma_{31} + R_1^\dagger \sigma_{13}) + \lambda_2 (R_2 \sigma_{32} + R_2^\dagger \sigma_{23}). \quad (2)$$

Here, $\sigma_{ij} = |i\rangle \langle j|$ where $|j\rangle$ is an atomic state, $\{\omega_j\}$ are positive constants, χ_i represents the strength of the nonlinearity in the field F_i , and λ_1, λ_2 are the respective atom-field coupling strengths corresponding to the $|3\rangle \leftrightarrow |1\rangle$ and $|3\rangle \leftrightarrow |2\rangle$ transitions. Further,

$$R_i = a_i f(N_i), \quad (3)$$

where $f(N_i)$ is a real-valued function of $N_i = a_i^\dagger a_i$ that serves to incorporate a possible intensity-dependent coupling. As stated in the Introduction, we consider the functional form $f(N_i) = (1 + \kappa_i N_i)^{1/2}$, where κ_i takes values in the range $[0, 1]$. Wherever relevant, a comparison will be made with results pertinent to the cases $f(N_i) = 1$ and $f(N_i) = N_i^{1/2}$. H can be written as the sum $H_0 + H_1$, where

$$H_0 = \sum_{i=1}^2 \Omega_i N_i^{\text{tot}} + \omega_3 I, \quad (4a)$$

$$H_1 = \sum_{i=1}^2 \chi_i a_i^{\dagger 2} a_i^2 - \Delta_i \sigma_{ii} + \lambda_i (R_i \sigma_{3i} + R_i^\dagger \sigma_{i3}). \quad (4b)$$

Here $I = \sum_{j=1}^3 \sigma_{jj}$, $N_i^{\text{tot}} = a_i^\dagger a_i - \sigma_{ii}$ ($i = 1, 2$) are constants of the motion, and the two detuning parameters Δ_i are given by

$$\Delta_i = \omega_3 - \omega_i - \Omega_i. \quad (5)$$

H_0 merely introduces a phase factor in the time evolution of the state. It is therefore convenient to work in an appropriate interaction picture to eliminate this trivial dependence.

Earlier work [27] pertaining to a Λ atom interacting with two radiation fields involved an intensity-dependent coupling specified by $f(N_i) = N_i^{1/2}$, and a cross-Kerr nonlinearity between the fields, but not individual field nonlinearities as in the present instance. Entanglement collapse to a constant value over a significant time interval has not been reported hitherto, nor has EIT been examined in this case. The model we consider here provides a natural setting for examining the effects of individual field nonlinearities, detuning parameters, a family of intensity-dependent couplings and specific classes of initial states on EIT and entanglement dynamics during temporal evolution.

The quantities we require for our study are the matrix elements of the time-dependent reduced density matrices of the tripartite system. We consider F_1 and F_2 to be initially in general superpositions of Fock states, $\sum_0^\infty q_n |n\rangle$ and $\sum_0^\infty r_m |m\rangle$, respectively. For definiteness, the initial state of the atom is taken to be $|1\rangle$ throughout. The initial state of the full system is thus

$$|\psi(0)\rangle = \sum_{n=0}^{\infty} \sum_{m=0}^{\infty} q_n r_m |1; n; m\rangle, \quad (6)$$

where $|1; n; m\rangle$ denotes a state with the atom in $|1\rangle$ and the fields F_1 and F_2 in states with n and m photons, respectively. (An analogous notation will be used for other field states as well, such as coherent and photon-added coherent states.) Proceeding on lines similar to those for the V atom [18], the interaction picture state vector at time t is found to be

$$\begin{aligned} |\psi(t)\rangle_{\text{int}} = & \sum_{n=0}^{\infty} \sum_{m=0}^{\infty} q_n r_m \left\{ A_{nm}(t) e^{i\Delta_1 t} |1; n; m\rangle \right. \\ & + B_{nm}(t) e^{i\Delta_2 t} |2; n-1; m+1\rangle \\ & \left. + C_{nm}(t) |3; n-1; m\rangle \right\}, \end{aligned} \quad (7)$$

where the functions $A_{nm}(t)$, $B_{nm}(t)$, $C_{nm}(t)$ are as follows. Since the atom is taken to be initially in the state $|1\rangle$, it cannot make a transition to $|3\rangle$ if $n = 0$. Hence

$$A_{0m}(t) = 1, \quad B_{0m}(t) = C_{0m}(t) = 0 \quad (8)$$

for all m . When $n, m \geq 1$, we find

$$\begin{aligned} A_{nm}(t) = & \frac{e^{i(\Delta_2 - \Delta_1)t}}{f_1 f_2} \sum_{j=1}^3 b_j \left\{ (\Delta_2 + \mu_j + V_{12} + V_{22}) \right. \\ & \left. + (\mu_j + V_{12} + V_{21}) - f_2^2 \right\} e^{i\mu_j t}, \end{aligned} \quad (9a)$$

$$B_{nm}(t) = \sum_{j=1}^3 b_j e^{i\mu_j t}, \quad (9b)$$

$$C_{nm}(t) = -\frac{e^{i\Delta_2 t}}{f_2} \sum_{j=1}^3 b_j (\mu_j + V_{12} + V_{21}) e^{i\mu_j t}, \quad (9c)$$

where

$$V_{11} = \chi_1 n(n-1), \quad V_{12} = \chi_1 (n-1)(n-2), \quad (10a)$$

$$V_{21} = \chi_2 m(m+1), \quad V_{22} = \chi_2 m(m-1), \quad (10b)$$

$$f_1 = \lambda_1 n^{1/2} f(n), \quad f_2 = \lambda_2 (m+1)^{1/2} f(m+1). \quad (10c)$$

The effect of the operator $f(N)$ in the Hamiltonian on the state of the system is captured in the quantities f_1 and f_2 . Further,

$$\mu_j = -\frac{1}{3} x_1 + \frac{2}{3} (x_1^2 - 3x_2)^{1/2} \cos \left\{ \theta + \frac{2}{3} (j-1)\pi \right\} \quad (11)$$

where $j = 1, 2, 3$, and

$$\theta = \frac{1}{3} \cos^{-1} \left\{ [9x_1 x_2 - 2x_1^3 - 27x_3] / [2(x_1^2 - 3x_2)^{3/2}] \right\}, \quad (12)$$

$$x_1 = V_{11} + 2V_{12} + V_{21} + 2V_{22} - \Delta_1 + 2\Delta_2, \quad (13a)$$

$$\begin{aligned} x_2 = & (V_{12} + V_{21} + \Delta_2)(V_{11} + V_{12} + 2V_{22} - \Delta_1) \\ & + (V_{12} + V_{22})(V_{11} + V_{22} - \Delta_1) + 2\Delta_2(V_{12} + V_{21}) \\ & + \Delta_2^2 - f_1^2 - f_2^2, \end{aligned} \quad (13b)$$

$$\begin{aligned} x_3 = & \Delta_2(V_{12} + V_{21})(V_{11} + V_{12} + 2V_{22} - \Delta_1) \\ & - f_2^2(V_{11} + V_{22} - \Delta_1 + \Delta_2) + \Delta_2^2(V_{12} + V_{21}) \\ & + (V_{12} + V_{21}) \left\{ (V_{12} + V_{22})(V_{11} + V_{22} - \Delta_1) - f_1^2 \right\}, \end{aligned} \quad (13c)$$

and

$$b_j = f_1 f_2 / [(\mu_j - \mu_k)(\mu_j - \mu_l)], \quad j \neq k \neq l. \quad (14)$$

Finally, for $m = 0$ we find

$$A_{n0}(t) = \sum_{j=1}^2 c_j e^{i\alpha_j t}, \quad (15a)$$

$$B_{n0}(t) = 0, \quad (15b)$$

$$C_{n0}(t) = -\frac{e^{i\Delta_1}}{f_1} \sum_{j=1}^2 c_j (\alpha_j + V_{11}) e^{i\alpha_j t}, \quad (15c)$$

where

$$c_1 = \frac{V_{11} + \alpha_2}{\alpha_2 - \alpha_1}, \quad c_2 = \frac{V_{11} + \alpha_1}{\alpha_1 - \alpha_2} \quad (16)$$

and

$$\alpha_{1,2} = \frac{1}{2}[-y_1 \pm (y_1^2 - 4y_2)^{1/2}], \quad (17)$$

where

$$y_1 = V_{11} + V_{12}, \quad y_2 = V_{12}V_{11} - f_1^2. \quad (18)$$

In the expressions for $B_{nm}(t)$ in the foregoing, the contribution from spontaneous emission has not been included, as it can be shown to be negligible.

With these results at hand, the general matrix elements of the reduced density matrices $\rho_1(t)$, $\rho_2(t)$ and $\rho_a(t)$ for the field subsystems F_1 , F_2 and the atom subsystem, respectively, can be computed by tracing over the other two subsystems. We obtain, finally,

$$\begin{aligned} \langle n | \rho_1(t) | n' \rangle = & \sum_{l=0}^{\infty} \left[q_n q_{n'}^* r_l r_l^* A_{n,l} A_{n',l}^* + q_{n+1} q_{n'+1}^* r_l r_l^* C_{n+1,l} C_{n'+1,l}^* \right. \\ & \left. + (1 - \delta_{l,0})(q_{n+1} q_{n'+1}^* r_{l-1} r_{l-1}^* B_{n+1,l-1} B_{n'+1,l-1}^*) \right], \end{aligned} \quad (19)$$

$$\begin{aligned} \langle l | \rho_2(t) | l' \rangle = & \sum_{n=0}^{\infty} \left[q_n q_n^* r_l r_l^* A_{n,l} A_{n,l}^* + q_{n+1} q_{n+1}^* r_l r_l^* C_{n+1,l} C_{n+1,l}^* \right. \\ & \left. + (1 - \delta_{l,0})(1 - \delta_{l',0})(q_{n+1} q_{n+1}^* r_{l-1} r_{l-1}^* B_{n+1,l-1} B_{n+1,l'-1}^*) \right], \end{aligned} \quad (20)$$

and

$$\langle 1 | \rho_a(t) | 1 \rangle = \sum_{k=0}^{\infty} \sum_{l=0}^{\infty} q_k q_k^* r_l r_l^* A_{k,l} A_{k,l}^*, \quad (21a)$$

$$\langle 2 | \rho_a(t) | 2 \rangle = \sum_{k=0}^{\infty} \sum_{l=1}^{\infty} q_{k+1} q_{k+1}^* r_{l-1} r_{l-1}^* B_{k+1,l-1} B_{k+1,l-1}^*, \quad (21b)$$

$$\langle 3 | \rho_a(t) | 3 \rangle = \sum_{k=0}^{\infty} \sum_{l=0}^{\infty} q_{k+1} q_{k+1}^* r_l r_l^* C_{k+1,l} C_{k+1,l}^*, \quad (21c)$$

$$\langle 1 | \rho_a(t) | 2 \rangle = \sum_{k=0}^{\infty} \sum_{l=1}^{\infty} q_k q_{k+1}^* r_l r_{l-1}^* A_{k,l} B_{k+1,l-1}^*, \quad (21d)$$

$$\langle 1 | \rho_a(t) | 3 \rangle = \sum_{k=0}^{\infty} \sum_{l=0}^{\infty} q_k q_{k+1}^* r_l r_l^* A_{k,l} C_{k+1,l}^*, \quad (21e)$$

$$\langle 2 | \rho_a(t) | 3 \rangle = \sum_{k=0}^{\infty} \sum_{l=1}^{\infty} q_{k+1} q_{k+1}^* r_{l-1} r_l^* B_{k+1,l-1} C_{k+1,l}^*. \quad (21f)$$

The quantity of interest in the context of EIT (to be analysed in the next section) is the expectation value of the photon number of the probe field F_1 , given by

$$\langle N_1(t) \rangle = \text{Tr} [\rho_1(t) N_1], \quad (22)$$

while entanglement dynamics (examined in section 4) is characterised by the SVNE of the atomic subsystem, defined as

$$S_a(t) = -\text{Tr} [\rho_a(t) \ln \rho_a(t)]. \quad (23)$$

3. Electromagnetically-induced transparency (EIT)

We are ready, now, to investigate EIT for a Λ atom interacting with the probe field F_1 and the coupling field F_2 . In order to have a reference point from which to understand the general behaviour, we consider first the relatively simple case in which the detuning parameter $\Delta_2 = 0$, the couplings $\lambda_1 = \lambda_2 = \lambda = 1$, and the field nonlinearity parameters $\chi_1 = \chi_2 = 0$. As mentioned earlier, we consider situations where $\langle N_1 \rangle$ exhibits collapses and revivals during the temporal evolution of the system, and examine features of EIT during that particular interval of time when $\langle N_1 \rangle$ first collapses to a constant value in the absence of F_2 .

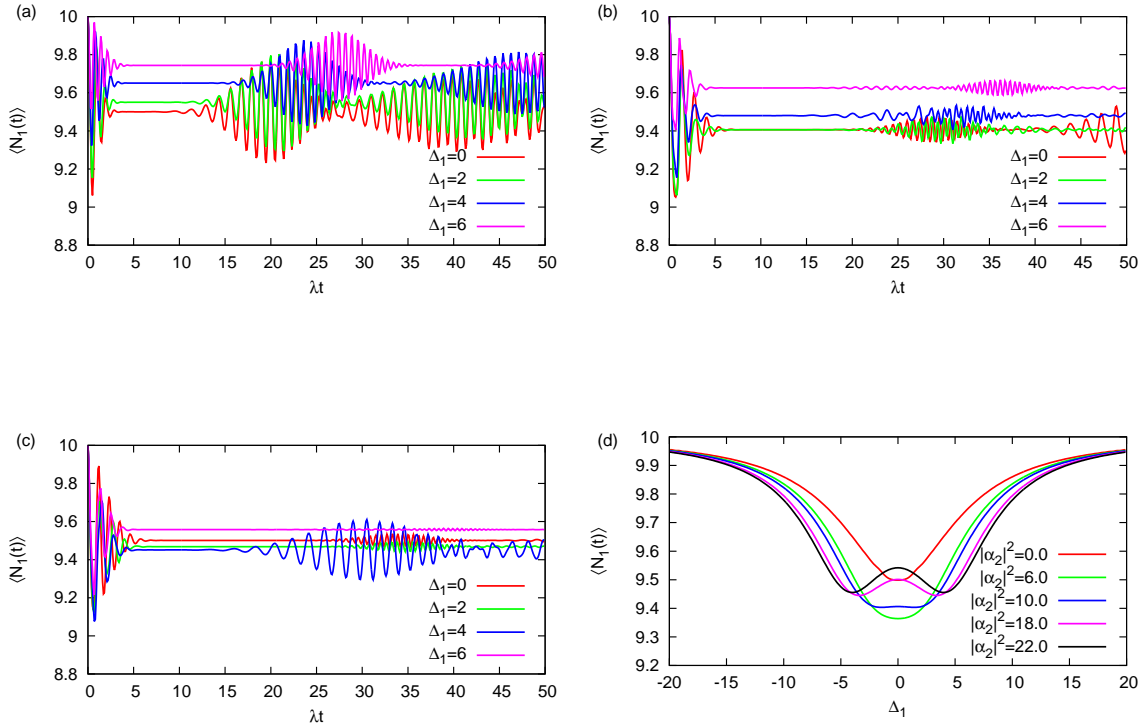


Figure 1: $\langle N_1(t) \rangle$ in the case of initial coherent states $|\alpha_1\rangle$ and $|\alpha_2\rangle$ of the field modes. $|\alpha_1|^2 = 10$ and (a) $|\alpha_2|^2 = 0$, (b) $|\alpha_2|^2 = 10$, (c) $|\alpha_2|^2 = 18$. (d) $\langle N_1 \rangle$ as a function of the detuning parameter Δ_1 , for different values of $|\alpha_2|^2$.

When the initial states of F_1 and F_2 are coherent states $|\alpha_1\rangle$ and $|\alpha_2\rangle$, $\langle N_1(t) \rangle$ undergoes collapses and revivals in time for a range of values of Δ_1 and $|\alpha_2|^2$, for a given value of $|\alpha_1|^2$ (figures 1(a)-(c)). The time interval over which $\langle N_1 \rangle$ exhibits collapse is sensitive to the values of both Δ_1 and $|\alpha_1|^2$. Since the intervals of first collapse for different values of Δ_1 overlap with each other, we can capture the appearance of EIT in a plot of $\langle N_1(t) \rangle$ versus Δ_1 at any specific instant of time in this overlap interval (figure 1(d)). In particular, the generation of a transparency window around $\Delta_1 = 0$ for

$|\alpha_2|^2 \gg |\alpha_1|^2$ is manifest. We have also verified that the occupation probabilities of the atomic states $|1\rangle$ and $|3\rangle$ appropriately complement the behaviour of $\langle N_1 \rangle$ in this time interval.

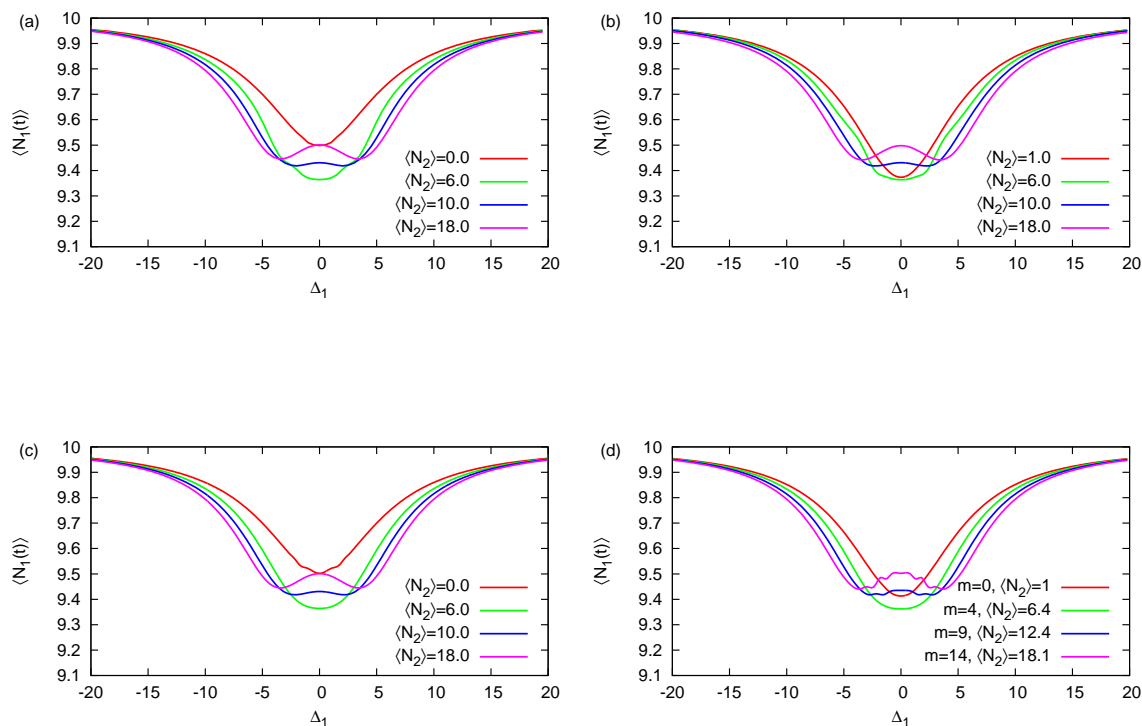


Figure 2: $\langle N_1(t) \rangle$ versus Δ_1 , when the initial state of F_2 is (a) an even CS (b) an odd CS, (c) a Yurke-Stoler state (d) an m -photon-added CS.

We now proceed to examine the effect of field nonlinearities, intensity-dependent couplings and different initial states of the coupling field on EIT. As before, we take F_1 to be initially in a CS with $|\alpha_1|^2 = 10$, and set $\chi_1 = \chi_2 = 0$, $\Delta_2 = 0$, $\lambda_1 = \lambda_2 = \lambda = 1$, while the initial state of F_2 is chosen to be an m -PACS or a Schrödinger cat state. Once again, EIT occurs during the first interval of collapse of $\langle N_1(t) \rangle$ (figures 2(a)-(c)). The height of the transparency window in the absorption spectrum now depends directly on $\langle N_2 \rangle$, consistent with the experimental finding [6]. When the initial state of F_2 is an m -PACS (as opposed to a CS), then, with increasing m , the field mode undergoes incomplete collapses which have Rabi-like oscillations about a mean value. This is reflected in the jaggedness of the transparency peak for large values of m (figure 2(d)). For very large values of m the intervals of collapse corresponding to different values of Δ_1 no longer overlap significantly, consistent with what happens when F_2 is initially in a photon number state.

The presence of nonlinearities in F_1 mitigates collapses of $\langle N_1(t) \rangle$. On the other hand, if F_2 has a Kerr-like nonlinearity, complete collapses in $\langle N_1(t) \rangle$ occur.

We investigate the nature of EIT during the time interval of the first collapse by choosing initial coherent states with $|\alpha_1|^2 = 10$ and $|\alpha_2|^2 = 18$ for F_1 and F_2 , setting $\lambda_1 = \lambda_2 = \lambda = 1$, $\chi_1 = 0$, and varying χ_2 . The EIT spectrum (a plot of $\langle N_1(t) \rangle$ versus Δ_1) is no longer symmetric about $\Delta_1 = 0$, in contrast to the earlier case, and the asymmetry becomes more pronounced with increasing χ_2 . A noteworthy feature is that this behaviour is similar to that obtained by varying Δ_2 over a small range of values about zero (figures 3(a), (b)).

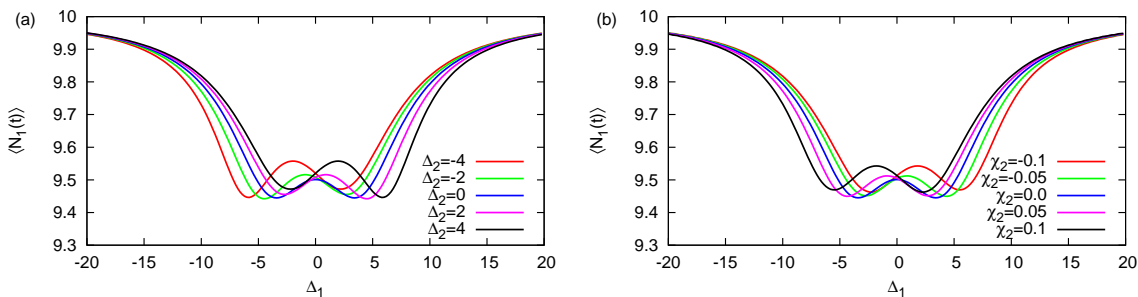


Figure 3: EIT spectrum for different values of (a) Δ_2 and (b) χ_2 .

Finally, if the coupling between the atom and either of the two fields has an intensity dependence of the form $f(N) = (1 + \kappa N)^{1/2}$, the EIT spectrum stretches and flattens out with increasing κ . Figure 4 illustrates this feature in the case of initial coherent states of F_1 and F_2 with $|\alpha_1|^2 = 10$, $|\alpha_2|^2 = 18$. Unlike what happens for non-zero values of χ_2 or Δ_2 , however, the spectrum remains symmetric about $\Delta_1 = 0$ as κ is increased, while the minima in $\langle N_1(t) \rangle$ that indicate EIT become less pronounced and move out to larger and larger values of $|\Delta_1|$.

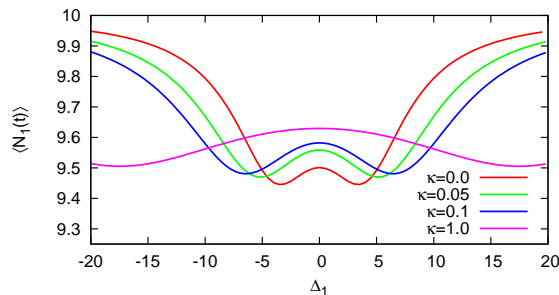


Figure 4: EIT spectrum for different values of κ .

4. Entanglement dynamics of a Λ atom coupled to two field modes

We turn, next, to the entanglement dynamics of our tripartite system. We start with the simple case of an intensity-independent field-atom coupling, and then go on to consider the case of an intensity-dependent coupling proportional to $(1+\kappa N)^{1/2}$. In order to avoid inessential complications, we set $\Delta_1 = \Delta_2 = \Delta$, $\lambda_1 = \lambda_2 = \lambda$, $\chi_1 = \chi_2 = \chi$, and $\kappa_1 = \kappa_2 = \kappa$.

4.1. Field-atom interactions with constant coupling strengths

Earlier work [17] has indicated an interesting feature in the behaviour of the entanglement in the system as measured by $S_a(t)$, the SVNE of the atomic subsystem, when the nonlinearity parameter χ is large compared to the field-atom interaction strength λ . In this regime, S_a displays a collapse (to a steady value) when the initial field state is a PACS, in contrast to what happens when it is a CS. This feature has been verified in detail for the system at hand, and figures 5(a) and (b) depict some representative results in this regard. With an increase in the number of added photons in the initial field states, there is a systematic increase of the interval during which S_a remains at a steady value. We have verified that these features are also reflected in the Mandel Q parameter and in the mean and variance of the photon number N_1 .

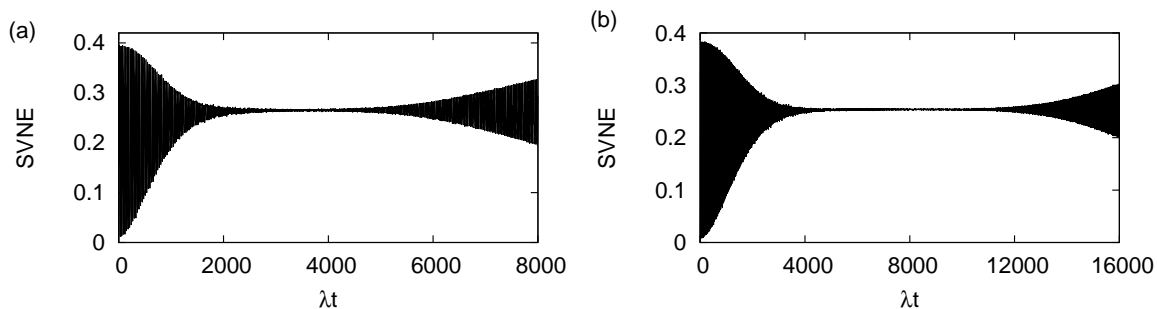


Figure 5: $S_a(t)$ for a Λ atom interacting with two field modes, for $\chi/\lambda = 5$, $\Delta = 0$. Initial state (a) $|1; \alpha, 5; \alpha, 5\rangle$ and (b) $|1; \alpha, 10; \alpha, 10\rangle$, with $|\alpha|^2 = 10$.

The time interval during which the SVNE holds at a steady value is enhanced when $|\alpha|^2$ is increased (compare figures 5(a) and 6(a)), or the ratio χ/λ is increased (see, e.g., figures 5(a) and 6(b)), or both, all other parameters remaining unchanged. This sort of entanglement collapse is absent in the case of initial coherent states, and also for initial PACS provided the nonlinearity parameter χ is sufficiently small [17]. The route to entanglement collapse with increase in nonlinearity is evident by comparing figures 7(a) and (b) with figure 5(a). As one might expect, there is a shrinkage of the time interval over which the entanglement collapses as one moves away from exact resonance

to non-zero values of the detuning parameters Δ_i .

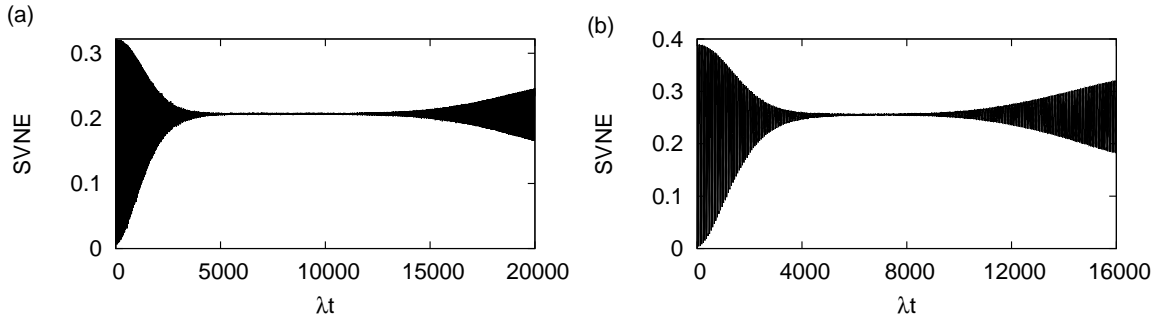


Figure 6: $S_a(t)$ for the initial state $|1; \alpha, 5; \alpha, 5\rangle$, where (a) $|\alpha|^2 = 20$ and $\chi/\lambda = 5$; (b) $|\alpha|^2 = 10$ and $\chi/\lambda = 10$ (strong nonlinearity). In both cases, $\Delta = 0$.

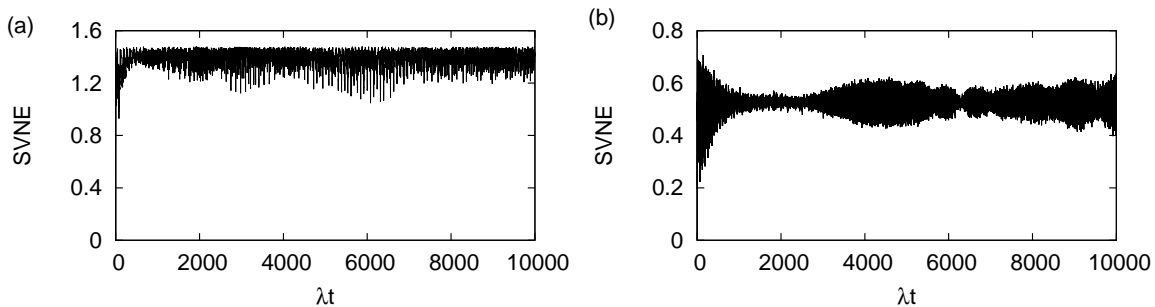


Figure 7: $S_a(t)$ for the initial state $|1; \alpha, 5; \alpha, 5\rangle$ with $|\alpha|^2 = 10$ and (a) $\chi = 0$ and (b) $\chi/\lambda = 1$ (weak nonlinearity). In both cases, $\Delta = 0$.

For completeness, we have also investigated the role of squeezing on entanglement collapse in this model. No collapse is exhibited by S_a when F_1 is a standard squeezed vacuum state (labelled by the complex parameter ξ) and F_2 is either a PACS or a squeezed vacuum state (with the same parameter ξ). Figures 8(a) and (b) illustrate these conclusions. Moreover, we have verified that, for those initial states for which a collapse of S_a does occur, the field states do not exhibit squeezing or second-order squeezing during the time interval of the collapse. It would seem, therefore, that it is the extent of *coherence*, above all else, that is the primary determining factor in the occurrence of entanglement collapses in our model system.

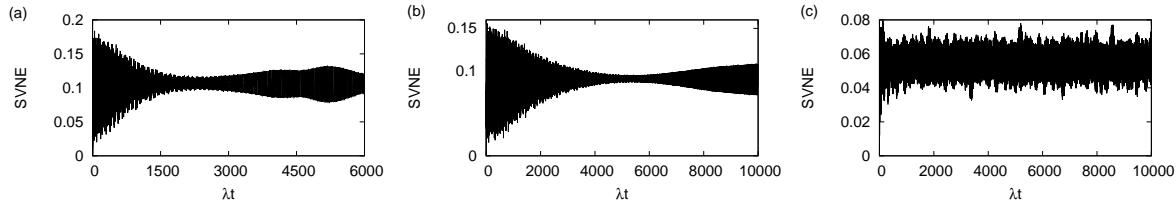


Figure 8: $S_a(t)$ in the presence of squeezing. Initial states (a) $|1; \xi; \alpha, 5\rangle$, (b) $|1; \xi; \alpha, 10\rangle$ and (c) $|1; \xi; \xi\rangle$, with $|\alpha|^2 = 10$ and squeezing parameter $\xi = 2$. In all cases, $\Delta = 0$ and $\chi/\lambda = 5$.

4.2. Intensity-dependent couplings: From SVNE collapse to the revival phenomenon

We turn, now, to the effect of an intensity-dependent coupling of the atom with the field modes, as characterised by a non-constant function $f(N_i)$ in (3).

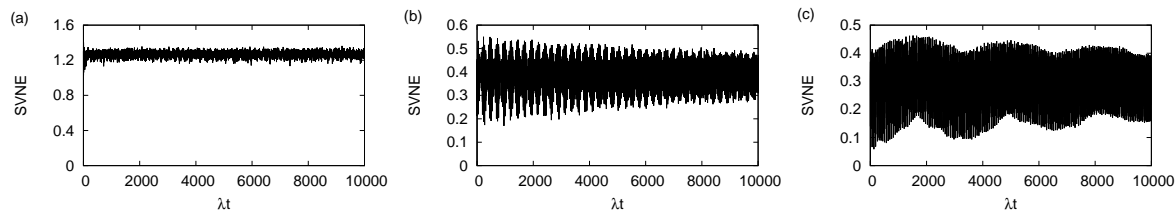


Figure 9: $S_a(t)$ for intensity-dependent coupling $f(N) = N^{1/2}$. Initial state $|1; \alpha, 5; \alpha, 5\rangle$, $|\alpha|^2 = 10$, $\Delta = 0$. (a) $\chi = 0$, (b) $\chi/\lambda = 6$, (c) $\chi/\lambda = 10$.

In order to facilitate ready comparison, we consider the same initial state, $|1; \alpha, 5; \alpha, 5\rangle$ with $|\alpha|^2 = 10$ and $\Delta = 0$, as in figures 5(a), 7(a) and 7(b). These correspond to intensity-independent coupling, i.e., $f(N_i) = 1$, for a range of values of χ/λ . Consider, now, the functional form [19] $f(N_i) = N_i^{1/2}$. Figures 9(a)-(c) depict the behaviour of $S_a(t)$ in this case. It is evident that SVNE collapse is absent now, even for strong nonlinearity. The behaviour in these two limiting cases motivates an examination of the effect of the intensity-dependent coupling $f(N_i) = (1 + \kappa N_i)^{1/2}$ over a range of values of the parameter κ , running from 0 to 1. Remarkably diverse features emerge, including SVNE collapse as well as recurrent collapses and revivals, as shown in figures 10(a)-(1). The behaviour is sensitively dependent on the value of κ .

The collapse of the SVNE over a considerable time interval that occurs for $\kappa = 0$ (figure 10(a)) is gradually lost (figures 10(b) to (e)) as κ increases to a value slightly above 0.005. An apparent precursor to collapse again appears as κ is further increased slightly (figure 10(f), $\kappa = 0.006$), but what happens is that there is a shorter-duration collapse, followed by a revival, and then a second incipient collapse and revival (figure

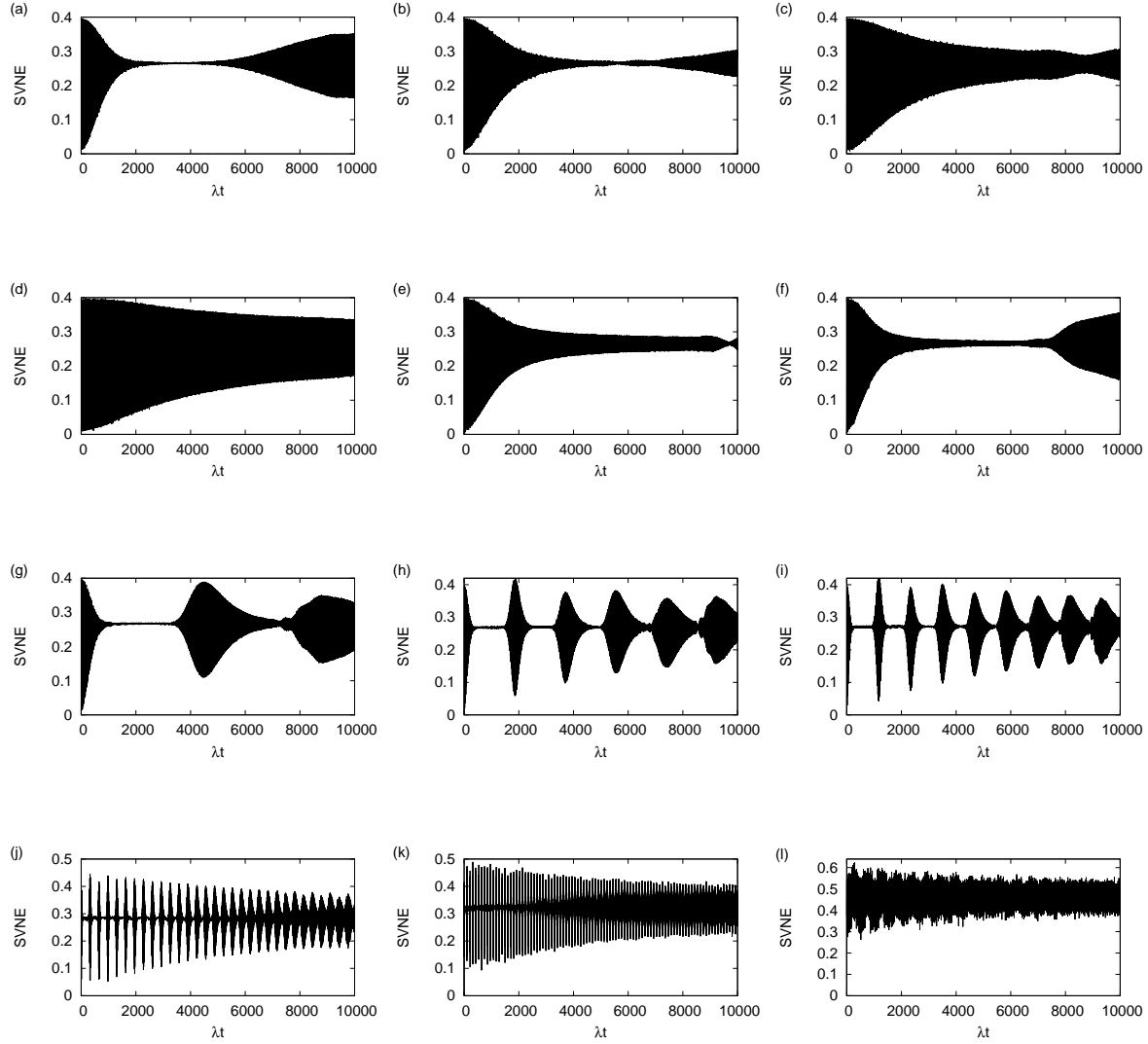


Figure 10: $S_a(t)$ for intensity-dependent coupling $f(N) = (1 + \kappa N)^{1/2}$. Initial state $|1; \alpha, 5; \alpha, 5\rangle$, $|\alpha|^2 = 10$, $\Delta = 0$, $\chi/\lambda = 5$. The value of κ is (a) 0, (b) 0.0012, (c) 0.002, (d) 0.0034, (e) 0.005, (f) 0.006, (g) 0.01, (h) 0.02, (i) 0.03, (j) 0.1, (k) 0.3 and (l) 1.

10(g), $\kappa = 0.01$), within the original time interval of collapse. A further small increase in κ produces a distinctive sequence of collapses and revivals (figures 10(h), (i), (j)), which remains clear-cut till κ becomes a little larger than 0.1. Subsequently, the intervals between successive revivals become too short to be discernible on the scale used in figure 10, and, moreover, fractional revivals start filling these small intervals (figure 10(k), $\kappa = 0.3$). As κ is increased further, the entanglement collapse and revival phenomenon is no longer discernible. Figure 10(l) depicts $S_a(t)$ for $\kappa = 1$. It is thus evident that a series of qualitative changes is exhibited by the entanglement entropy in the system under study as the value of κ is changed in a relatively small range, signalling very sensitive dependence on this parameter in a manner reminiscent of bifurcation cascades

preceding the onset of chaos in nonlinear classical dynamical systems.

Finally, as stated in the Introduction, we have verified that these interesting features are also exhibited in the case of a V atom interacting with two radiation modes.

5. Concluding remarks

We have considered a tripartite system comprising a Λ -type or V-type atom interacting with two radiation fields. The mean photon number corresponding to the probe field is seen to display collapses and revivals for specific initial field states and parameters in the Hamiltonian, in the absence of the coupling field. With the coupling field turned on, a window of electromagnetically-induced transparency appears during the collapse interval in the absorption spectrum. On a longer time scale, interesting dynamical effects are observed in the time evolution of the entanglement. This includes a collapse of the subsystem von Neumann entropy of the atom over a considerable time interval. Both these features are sensitive to the nature of the initial states of the fields, and seem to reflect the extent of the departure from coherence of those states.

We have attempted to identify the roles played by field nonlinearities, detuning parameters and the departure from coherence of the initial states of the radiation fields on EIT and on the extent of entanglement between subsystems during temporal evolution, since these two aspects are suitable for potential experimental investigations. Detailed experiments on EIT, the identification of the photon-added coherent state in the laboratory, and the necessity of retaining the extent of entanglement between subsystems from the point of view of quantum information processing add impetus to our investigations. Reconstruction of the state of the system during SVNE collapse could possibly be attempted through continuous-variable quantum state tomography. The unanticipated behaviour of the SVNE as the strength of the intensity-dependent field-atom coupling is varied would correspondingly take the system through a spectrum of nonclassical states which are worth identifying through state reconstruction procedures. The mean photon number is seen to reflect the long time dynamics of the SVNE corresponding to the atomic subsystem. This is an observable which lends itself to experimental observation, and hence one that can be used to examine the dynamical features predicted for the tripartite model considered.

References

- [1] Robinett R W 2004 *Phys. Rep.* **392** 1.
- [2] Milburn G J 1986 *Phys. Rev. A* **33** 674.
- [3] Kitagawa M and Yamamoto Y 1986 *Phys. Rev. A* **34** 3974.
- [4] Averbukh I Sh and Perelman N F 1989 *Phys. Lett. A* **139** 449.
- [5] Marangos J P 1998 *J. Mod. Opt.* **45** 471.
- [6] Boller K J, Imamoglu A and Harris S E 1991 *Phys. Rev. Lett.* **66** 2593.
- [7] Li Y and Xiao M 1995 *Phys. Rev. A* **51** R2703.
- [8] Éntin V M, Ryabtsev I I, Boguslavskii A E and Beterov I M 2000 *JETP Lett.* **71** 175.
- [9] Sudheesh C, Lakshmibala S and Balakrishnan V 2004 *Phys. Lett. A* **329** 14.

- [10] Sudheesh C, Lakshmibala S and Balakrishnan V 2005 *Europhys. Lett.* **71** 744.
- [11] Agarwal G S and Puri R R 1989 *Phys. Rev. A* **39** 2969.
- [12] Sudheesh C, Lakshmibala S and Balakrishnan V 2006 *J. Phys. B* **39** 3345.
- [13] Sudheesh C, Lakshmibala S and Balakrishnan V 2009 *Phys. Lett. A* **373** 2814.
- [14] Sudheesh C, Lakshmibala S and Balakrishnan V 2010 *EPL* **90** 50001.
- [15] Tara K, Agarwal G S and Chaturvedi S 1993 *Phys. Rev. A* **47** 5024.
- [16] Zavatta A, Viciani S and Bellini M 2004 *Science* **306** 660.
- [17] Athreya Shankar 2014 *Dynamics of field-atom interactions*, B. Tech. dissertation, IIT Madras (unpublished).
- [18] Athreya Shankar, Lakshmibala S and Balakrishnan V 2014 *J. Phys. B* **47** 215505.
- [19] Buck B and Sukumar C V 1981 *Phys. Lett. A* **81** 132.
- [20] Bužek V 1989 *Phys. Lett. A* **139** 231.
- [21] Bužek V 1989 *Phys. Rev. A* **39** 3196.
- [22] Zait R A 2003 *Phys. Lett. A* **319** 461.
- [23] Sudarshan E C G 1993 *Int. J. Th. Phys.* **32** 1069.
- [24] Sivakumar S 2004 *Int. J. Th. Phys.* **43** 2405.
- [25] Sivakumar S 2002 *J. Phys. A: Math. Gen.* **35** 6755.
- [26] Faghihi M J, Tavassoly M K and Harouni M B 2014 *Laser Phys.* **24** 045202.
- [27] Faghihi M J, Tavassoly M K and Hooshmandasl M R 2013 *J. Opt. Soc. Am. B* **30** 1109.